AMERICAN SOCIETY FOR MICROBIOLOGY | Journal of Bacteriology®

MEETING PRESENTATION

A Xylose-Inducible Expression System and a CRISPR Interference Plasmid for Targeted Knockdown of Gene Expression in *Clostridioides difficile*

Ute Müh,[a] Anthony G. Pannullo,[a] David S. Weiss,[a] Craig D. Ellermeier[a]

[a]Department of Microbiology and Immunology, University of Iowa, Iowa City, Iowa, USA

ABSTRACT Here we introduce plasmids for xylose-regulated expression and repression of genes in *Clostridioides difficile*. The xylose-inducible expression vector allows for ~100-fold induction of an *mCherryOpt* reporter gene. Induction is titratable and uniform from cell to cell. The gene repression plasmid is a CRISPR interference (CRISPRi) system based on a nuclease-defective, codon-optimized allele of the *Streptococcus pyogenes* Cas9 protein (*dCas9*) that is targeted to a gene of interest by a constitutively expressed single guide RNA (sgRNA). Expression of *dCas9* is induced by xylose, allowing investigators to control the timing and extent of gene silencing, as demonstrated here by dose-dependent repression of a chromosomal gene for a red fluorescent protein (maximum repression, ~100-fold). To validate the utility of CRISPRi for deciphering gene function in *C. difficile*, we knocked down the expression of three genes involved in the biogenesis of the cell envelope: the cell division gene *ftsZ*, the S-layer protein gene *slpA*, and the peptidoglycan synthase gene *pbp-0712*. CRISPRi confirmed known or expected phenotypes associated with the loss of FtsZ and SlpA and revealed that the previously uncharacterized peptidoglycan synthase PBP-0712 is needed for proper elongation, cell division, and protection against lysis.

IMPORTANCE *Clostridioides difficile* has become the leading cause of hospital-acquired diarrhea in developed countries. A better understanding of the basic biology of this devastating pathogen might lead to novel approaches for preventing or treating *C. difficile* infections. Here we introduce new plasmid vectors that allow for titratable induction (P_{xyl}) or knockdown (CRISPRi) of gene expression. The CRISPRi plasmid allows for easy depletion of target proteins in *C. difficile*. Besides bypassing the lengthy process of mutant construction, CRISPRi can be used to study the function of essential genes, which are particularly important targets for antibiotic development.

KEYWORDS *Clostridioides difficile*, *Clostridium difficile*, CRISPR interference, gene expression, genetics

Clostridioides (formerly *Clostridium*) *difficile* is a strictly anaerobic, Gram-positive opportunistic pathogen that has become the leading cause of health care-associated diarrhea (1). The symptoms are caused by toxins that damage the intestinal epithelium and can range in severity from mild diarrhea to life-threatening conditions such as pseudomembranous colitis and toxic megacolon (2–4). A recent study estimated that *C. difficile* causes close to ~500,000 infections and contributes to ~25,000 deaths per year in the United States (1, 5). The Centers for Disease Control and Prevention has classified *C. difficile* as an "urgent threat" to human health (6).

Genetic tools to study the physiology of *C. difficile* have become increasingly available; nevertheless, the repertoire remains limited. Investigators wishing to manip-

Citation Müh U, Pannullo AG, Weiss DS, Ellermeier CD. 2019. A xylose-inducible expression system and a CRISPR interference plasmid for targeted knockdown of gene expression in *Clostridioides difficile*. J Bacteriol 201:e00711-18. https://doi.org/10.1128/JB.00711-18.

Editor Victor J. DiRita, Michigan State University

Address correspondence to David S. Weiss, david-weiss@uiowa.edu, or Craig D. Ellermeier, craig-ellermeier@uiowa.edu.

For a commentary on this article, see https://doi.org/10.1128/JB.00089-19.

Received 20 November 2018
Accepted 3 February 2019
Accepted manuscript posted online 11 February 2019
Published 21 June 2019

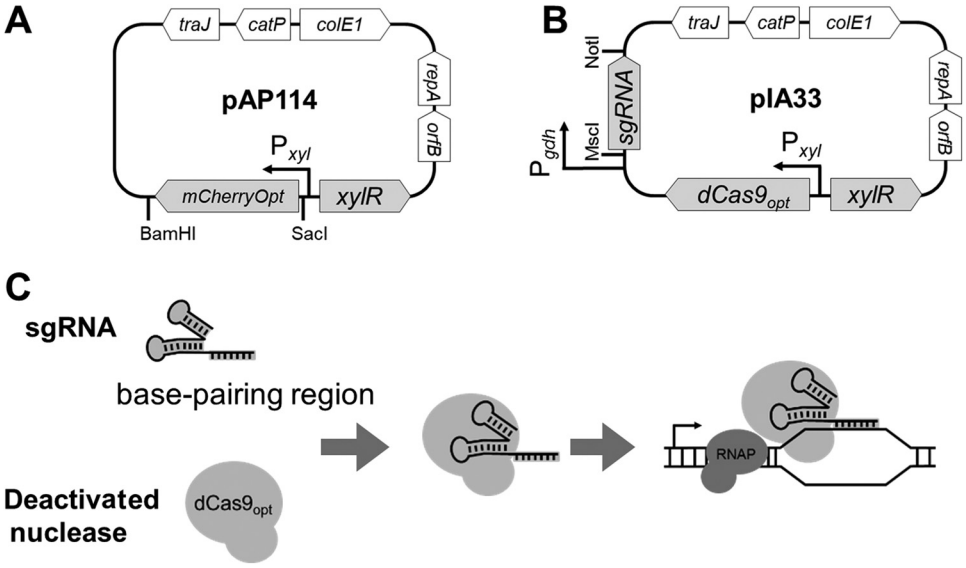

FIG 1 Genetic maps and CRISPRi principle. (A) pAP114 for xylose-inducible expression. The expression of the red fluorescent protein mCherryOpt is under P_{xyl} control. The gene can be replaced using the SacI and BamHI restriction sites. (B) pIA33 for CRISPRi. Single guide RNA (sgRNA) is under P_{gdh} control, and *dCas9* is under P_{xyl} control. The sgRNA sequence can be replaced using the MscI and NotI restriction sites. (C) CRISPRi principle. The deactivated nuclease binds sgRNA and is targeted to the gene of interest, but it is unable to cleave the DNA. Instead, dCas9 serves as a transcriptional roadblock. Features depicted are as follows: *mCherryOpt* encodes a red fluorescent protein variant that is codon optimized for expression in low-GC-content bacteria; *dCas9* encodes the deactivated CRISPR nuclease codon optimized for expression in low-GC-content bacteria; *orfB* and *repA* are the replication regions; *colE1* is the replication region of the *E. coli* plasmid pBR322 modified for a higher copy number; *catP* is the chloramphenicol acetyltransferase gene from *Clostridium perfringens*, conferring resistance to thiamphenicol in *C. difficile* or chloramphenicol in *E. coli*; and *traJ* encodes a conjugation transfer protein from plasmid RP4 (23). RNAP, RNA polymerase.

ulate gene expression have two options, a tetracycline-inducible promoter, P_{tet} (7), and a nisin-inducible promoter, P_{cpr} (8, 9). Although both systems are useful, the inducers, anhydrotetracycline and nisin, can inhibit growth (8, 10). This can make it difficult to deconvolute the effects of the inducer from the effects of altered gene expression. Investigators wishing to construct targeted knockouts in *C. difficile* have several options (11–13), but none of these can be applied to determine the function of essential genes, and even in the case of nonessential genes, the effort required to construct and validate mutants remains a significant bottleneck.

Here we describe two new plasmids that address some of these limitations. The first is a xylose-inducible expression vector based on the native P_{xyl} promoter of *C. difficile* (pAP114) (Fig. 1A). Similar xylose-inducible expression vectors have been developed for a number of bacteria (14–16), including one for *Clostridium perfringens* that is based on the *C. difficile* xylose-regulatory system (17). The xylose-inducible vector allows for uniform, tunable expression of an *mCherryOpt* reporter gene, with a maximum induction ratio of >100-fold.

The second new plasmid is a CRISPR interference (CRISPRi) vector that allows investigators to quickly assess the function of target genes, including essential genes, by blocking their expression (pIA33) (Fig. 1B). CRISPRi has been used to explore gene function in a variety of bacteria (e.g., see references 18 to 22), and we modeled our plasmid after a CRISPRi tool developed for *Bacillus subtilis* (23). CRISPRi uses a single guide RNA (sgRNA) to deliver a nuclease-deactivated mutant of Cas9 (dCas9) to a gene of interest, thereby creating a roadblock that prevents transcription by RNA polymerase (Fig. 1C) (20). Targeting repression to a new gene is simply a matter of replacing the sgRNA. Because *dCas9* is expressed from P_{xyl}, investigators can use xylose to control the timing and extent of gene silencing. To validate the utility of the CRISPRi vector, we show that it can achieve tunable repression of a chromosomal gene for a red fluores-

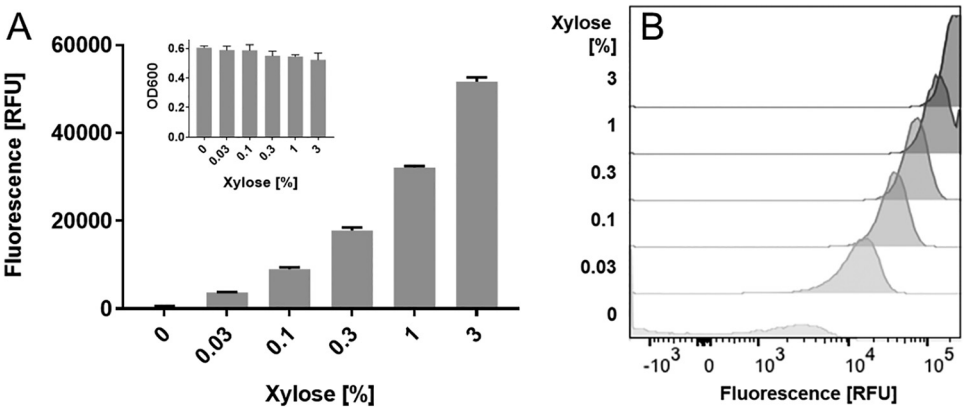

FIG 2 Tunable induction from P_{xyl} in R20291. A culture of R20291/pAP114 grown overnight was diluted to a starting OD_{600} of 0.05 into TY Thi_{10} medium with the indicated concentrations of xylose. Once cells had reached an OD_{600} of 0.5 (~5 h), they were fixed and processed to allow RFP development. (A) A plate reader was used to measure the relative fluorescence and OD_{600} of bulk samples. (B) Flow cytometry was used to measure the fluorescence of individual cells. RFU, relative fluorescence units normalized to the OD_{600}. Data in panel A represent the means and standard deviations of results from triplicate cultures. These results are representative of data from at least two independent experiments.

cent protein (RFP) (*rfp* gene) and document phenotypic defects caused by knocking down the expression of three genes that are critical for biogenesis of the cell envelope: *ftsZ*, *slpA*, and *cdr20291_0712*, which encodes a penicillin-binding protein (PBP) referred to here as PBP-0712.

RESULTS

Construction of a xylose-inducible expression system for *C. difficile*. To circumvent the deleterious effects of inducer toxicity inherent in the P_{tet} system (10), we constructed a xylose-inducible expression system. In *C. difficile*, the xylose gene cluster comprises the xylose repressor, *xylR* (*cdr20291_2900*), and the divergently transcribed catabolic genes *xylBA* (24). As determined in a variety of Gram-positive organisms, in the absence of xylose, XylR binds to the *xyl* operator (*xylO*) to repress transcription at P_{xyl} (24–26). To construct a xylose-inducible expression vector, we PCR amplified a 1.4-kb *xylR*-P_{xyl} DNA fragment from the chromosome of *C. difficile* strain R20291. This fragment was cloned upstream of a codon-optimized gene for the red fluorescent protein mCherry to create the P_{xyl}::*mCherryOpt* reporter plasmid named pAP114 (Fig. 1A).

R20291 harboring pAP114 exhibited a dose-dependent increase in red fluorescence when grown in medium containing increasing xylose concentrations, achieving an induction range of >100-fold (Fig. 2A). Flow cytometry revealed that the bacterial population was uniformly fluorescent over the full range of xylose concentrations (Fig. 2B). As expected, xylose did not inhibit growth even at the highest concentration tested, 3% (Fig. 2A, inset). Similar results were obtained when pAP114 was introduced into *C. difficile* strain 630Δ*erm* (see Fig. S1 in the supplemental material).

Expression of sugar utilization genes is often subject to carbon catabolite repression and in *C. difficile* is controlled by CcpA (27). Antunes et al. found that *xylA* expression was 3-fold lower in a *ccpA* mutant but was not subject to glucose repression (28). The *xylA* gene is located downstream of *xylB*. Thus, we sought to determine if the expression of P_{xyl} was subject to glucose repression. We found that xylose induction of P_{xyl} decreased by less than 40% in the presence of glucose, confirming that glucose does not play a major role in the regulation of this promoter (Fig. S2) (28).

Construction of a CRISPRi system for silencing gene expression in *C. difficile*. Peters et al. used knockdown of a chromosomal *rfp* allele expressed from the constitutive P_{veg} promoter to establish a CRISPRi system for *B. subtilis* (23). We took advantage of their P_{veg}::*rfp* construct and *rfp*-targeting sgRNA to establish an analogous CRISPRi

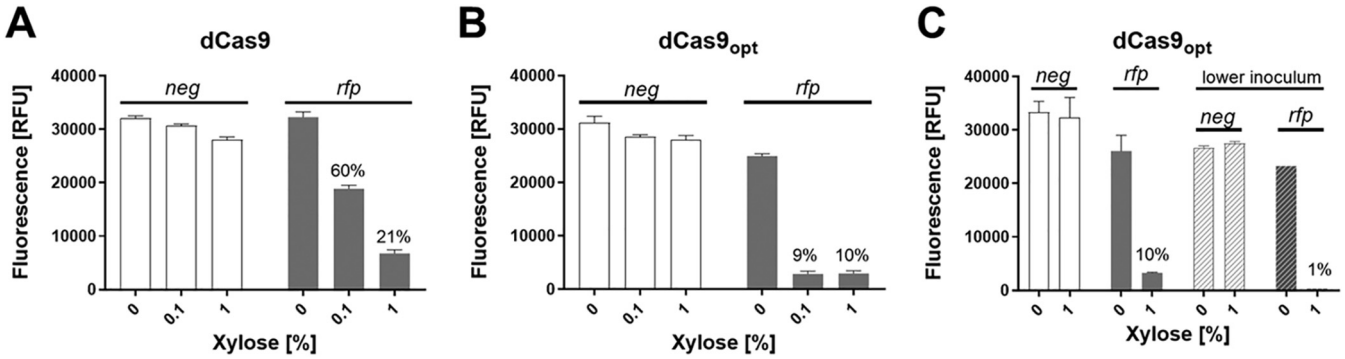

FIG 3 Suppression of *rfp* expression by CRISPRi. A set of CRISPRi plasmids was introduced into a *C. difficile* strain that expresses *rfp* constitutively. The CRISPRi plasmids express sgRNAs constitutively under P_{gdh} control and *dCas9* alleles under P_{xyl} control. Cultures grown overnight were diluted into TY Thi_{10} medium containing xylose, as indicated. When cultures reached an OD_{600} of 0.5 (~5 h), cells were fixed and processed to allow RFP development. (A) Cultures were inoculated to a starting OD_{600} of 0.05, and the CRISPRi plasmids expressed *dCas9* together with rfp^{sgRNA} or neg^{sgRNA} (negative control). (B) The *dCas9* gene was replaced with a codon-optimized *dCas9* gene. (C) The same CRISPRi plasmids as in panel B but with cultures inoculated to a starting OD_{600} of 0.05 or 0.01 (lower inoculum). Data are graphed as the means and standard deviations of data from triplicate cultures and are representative of results from at least two independent experiments. The host strain was UM275. The plasmids were pAI25 (P_{gdh}::neg^{sgRNA} P_{xyl}::*dCas9*), pAI28 (P_{gdh}::rfp^{sgRNA} P_{xyl}::*dCas9*), pAI33 (P_{gdh}::rfp^{sgRNA} P_{xyl}::*dCas9-opt*), and pAI34 (P_{gdh}::neg^{sgRNA} P_{xyl}::*dCas9-opt*).

system for *C. difficile*. (Note that this *rfp* allele is different from the *mCherryOpt rfp* allele described above to study xylose induction in pAP114.) Our first step was to construct a reporter strain by integrating P_{veg}::*rfp* downstream of *pyrE* to create strain UM275 (*C. difficile* 630Δ*erm* P_{veg}::*rfp*).

We then constructed a series of *Escherichia coli-C. difficile* shuttle vectors that expressed *Streptococcus pyogenes dCas9* under the control of P_{xyl} and the *rfp*-targeted sgRNA (rfp^{sgRNA}) under the control of various constitutive promoters: P_{veg}, P_{sigA}, and P_{gdh} (12, 23, 29). As a negative control, we used a pseudo-sgRNA with 20 nucleotides (nt) that does not anneal next to a protospacer adjacent motif (PAM) site (P_{gdh}::neg^{sgRNA}). The plasmids were conjugated into the reporter strain, and gene silencing was quantified by measuring red fluorescence with and without induction of *dCas9*. The RFP signal was reduced by each of the three constructs that expressed the *rfp*-targeting sgRNA but not by the negative control (Fig. S3). Inhibition correlated with the concentration of xylose (i.e., induction of *dCas9*) and was strongest when the sgRNA was cloned behind P_{veg} and P_{gdh}. We chose to continue with P_{gdh} where maximal inhibition was about 80% with 1% xylose (Fig. 3A and Fig. S3).

We achieved further improvement by replacing the *dCas9* gene with one that had been codon optimized for *C. difficile* (12) to create pIA33 (Fig. 1B). This final construct achieved 90% suppression of red fluorescence (Fig. 3B) when the reporter strain was grown for ~3 mass doublings (optical density at 600 nm [OD_{600}] of 0.05 to 0.5). The residual 10% RFP signal likely reflects carryover from the inoculum, in which case the true repression would be greater than 90%. Consistent with this inference, reducing the inoculum lowered the residual fluorescence to ~1% (Fig. 3C).

Applications of CRISPRi to study gene function in *C. difficile*. Once we optimized the CRISPRi plasmid against RFP, we tested its utility for studies of gene function by targeting three genes that play important roles in the assembly of the cell envelope: *ftsZ*, *slpA*, and *cdr20291_0712* (*pbp-0712*). These genes were considered good candidates for CRISPRi because they are not cotranscribed with other genes (30, 31), minimizing concerns with polarity. Moreover, all three were identified as being essential by saturation transposon mutagenesis (32), although a mutant lacking *slpA* was subsequently isolated by a different approach (33).

CRISPRi targeting *ftsZ*. FtsZ is a key division protein found in almost all bacteria (34, 35). Depletion of FtsZ in rod-shaped bacteria prevents division, leading to the formation of long filaments that eventually lyse. The appearance of highly filamentous cells provides a simple visual readout that has been used to demonstrate successful inhibition of *ftsZ* expression by CRISPRi in *E. coli* (36, 37), *B. subtilis* (23), and *Pseudomo-*

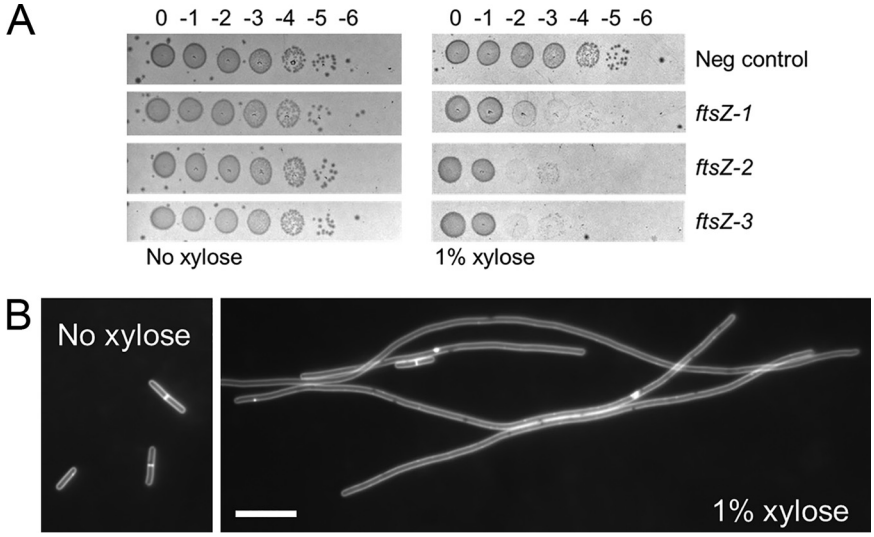

FIG 4 CRISPRi knockdown of *ftsZ*. (A) Viability assay. Cells of strain R20291 harboring CRISPRi plasmids were grown overnight in TY Thi_{10} medium. Samples were serially diluted, and 5 μl of each dilution was spotted onto TY Thi_{10} plates with or without 1% xylose to induce the expression of *dCas9-opt*. Plates were photographed after incubation overnight. The negative control was pIA34 (*neg*^{sgRNA}), while the plasmids that target *ftsZ* were pIA35 (*ftsZ-1*^{sgRNA}), pIA36 (*ftsZ-2*^{sgRNA}), and pIA37 (*ftsZ-3*^{sgRNA}). (B) Cell morphology. A culture of R20291/pAI35 (*ftsZ-1*^{sgRNA}) grown overnight was diluted to a starting OD_{600} of 0.05 in TY Thi_{10} medium with or without 1% xylose and grown for 4 h. Cells were stained with the membrane dye FM4-64 to reveal whether division septa were present and photographed under fluorescence. Bar = 10 μm. These results are representative of data from two independent experiments.

nas aeruginosa (22). In the coccus *Streptococcus pneumoniae*, CRISPRi knockdown of *ftsZ* expression causes swelling rather than filamentation (19).

We constructed three CRISPRi plasmids with different sgRNAs targeting *ftsZ* and conjugated these plasmids into strain R20291. All three constructs showed a strong growth inhibition phenotype, with an ~100- to 1,000-fold loss in viability when serial dilutions of a culture grown overnight (stationary phase) were spotted onto plates containing tryptone-yeast (TY) medium supplemented with thiamphenicol at 10 μg/ml (Thi_{10}) plus 1% xylose (Fig. 4A). Cells recovered from this plate were strikingly elongated, whereas the negative control exhibited normal morphology (Fig. S4). Liquid cultures of R20291 harboring one of the CRISPRi constructs were grown in the presence and absence of xylose and examined by microscopy after 4 h of induction. Knockdown of *ftsZ* expression produced filamentous cells that lacked cell division septa (Fig. 4B). Collectively, these findings indicate successful silencing of *ftsZ* expression by CRISPRi.

CRISPRi targeting *slpA*. The outermost layer of *C. difficile* is called the S-layer and consists of a two-dimensional paracrystalline array composed primarily of surface layer protein A (SlpA) (38, 39). SlpA is posttranslationally processed into a high-molecular-weight (HMW) and a low-molecular-weight (LMW) subunit that together form a tight heterodimeric complex which is incorporated into the S-layer (40, 41). It was initially thought that *slpA* might be essential since extensive transposon mutagenesis did not yield any insertions in *slpA* (32). However, growth in the presence of the SlpA-targeting bactericidal agent Avidocin selected for strains that lacked the ability to produce SlpA (33). An *slpA* mutant strain obtained by this selection method showed reduced sporulation and increased sensitivity to lysozyme and was attenuated in virulence (33). We set out to determine whether CRISPRi knockdown of *slpA* expression would confirm the phenotypes described for the *slpA* mutant strain.

We constructed two CRISPRi plasmids with sgRNAs designed to prevent the expression of *slpA*. R20291 harboring these plasmids was grown to stationary phase in the presence of 1% xylose. To assess the extent of SlpA depletion, cell wall proteins were extracted with low-pH buffer, and samples were analyzed by SDS-PAGE. Based on the intensity of Coomassie staining, SlpA levels were reduced to less than 5% of

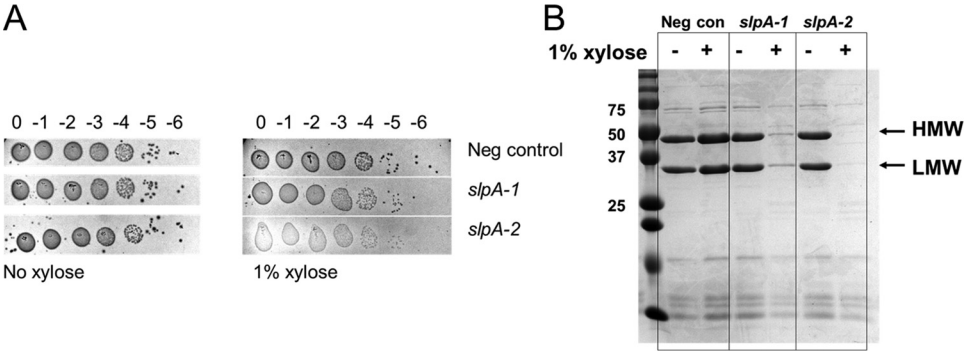

FIG 5 CRISPRi knockdown of *slpA*. (A) Viability assay as described in the legend to Fig. 4. CRISPRi constructs used in this experiment were pIA34 (*neg*^{sgRNA} [negative control]), pIA38 (*slpA-1*^{sgRNA}), and pIA39 (*slpA-2*^{sgRNA}). Note that sgRNAs targeting *slpA* produced small, translucent colonies that did not photograph well and were difficult to score, but growth was consistently observed out to the 10^{-5} dilution in all cases. (B) Extent of SlpA depletion. The same strains were diluted 1:50 into TY Thi$_{10}$ medium with or without 1% xylose. After growth for 8 h, cell wall proteins were extracted and analyzed by SDS-PAGE followed by Coomassie staining. Molecular mass markers in kilodaltons are indicated to the left. The high-molecular-weight (HMW) band and the low-molecular-weight (LMW) band of SlpA are marked. Results are representative of data from two experiments.

wild-type levels (Fig. 5B). Because SlpA-depleted cells tended to clump, which might affect the efficiency of cell wall protein extraction, we further verified extensive depletion of SlpA in whole-cell extracts (Fig. S5). Interestingly, the induced CRISPRi-*slpA* samples appear to lyse more readily during sample workup, as indicated by the higher levels of background bands.

CRISPRi knockdown of *slpA* in R20291 did not affect plating efficiency, although the colonies that grew were more translucent than the wild type (Fig. 5A). SlpA-depleted cells exhibited normal rod morphology under a phase-contrast microscope (Fig. S6). We found that knockdown of *slpA* expression led to increased lysozyme sensitivity in a growth curve at 0.2 mg/ml lysozyme (Fig. S7). Furthermore, the MIC for lysozyme was 8 to 16 mg/ml (Table 1) in a negative-control strain or an uninduced CRISPRi-*slpA* strain, which decreased to 4 mg/ml when the CRISPRi-*slpA* construct was induced. Finally, CRISPRi silencing of *slpA* reduced sporulation on TY Thi$_{10}$ plates about 1,000-fold (Table 2). Our findings are fully consistent with those reported previously for an *slpA*-null mutant obtained by selecting for resistance to Avidocin (33).

CRISPRi targeting *pbp-0712*. Penicillin-binding proteins (PBPs) are required to synthesize the peptidoglycan (PG) cell wall that surrounds most bacteria and protects them from lysis due to turgor pressure (42). Saturation transposon mutagenesis identified two PBPs as being essential in *C. difficile* (32). One of these, *cdr20291_0985*, is not very amenable to analysis by CRISPRi because it is embedded in an operon with homologs of numerous genes known to be essential for division and elongation in other rod-shaped bacteria, including *B. subtilis* and *E. coli*. The other, coding for PBP-0712 (*cdr20291_0712*), appears to be an isolated gene (30, 31). PBP-0712 is predicted to be a bifunctional (class A) PBP with both a glycosyltransferase domain for polymerization of glycan strands and a transpeptidase domain for cross-linking of adjacent stem peptides (43). Nothing is known about the specific roles of PBP-0712, such as whether it contributes primarily to elongation or division.

TABLE 1 Effect of CRISPRi knockdown of *slpA* on the MIC of lysozyme[a]

	MIC (mg/ml)	
Target	**No xylose**	**1% xylose**
neg^{sgRNA}	8	8
slpA-1^{sgRNA}	8–16	4
slpA-2^{sgRNA}	8–16	4

[a]Data are from two independent experiments.

TABLE 2 Effect of CRISPRi knockdown of *slpA* on sporulation[a]

Target	Spores (%)		Fold reduction
	No xylose	1% xylose	
neg^{sgRNA}	1.8	0.3	1
slpA-1^{sgRNA}	0.5	<0.002	>250
slpA-2^{sgRNA}	0.3	<0.0005	>600

[a]Data are the averages of results from two independent experiments.

To determine the phenotype of PBP-0712 depletion, two CRISPRi plasmids with sgRNAs targeting *pbp-0712* were introduced into R20291 by conjugation. Exconjugants plated onto TY Thi$_{10}$ plates containing 1% xylose exhibited an ~10^6-fold viability defect (Fig. 6A), confirming that *pbp-0712* is an essential gene. When inoculated at a starting OD_{600} of 0.05 and incubated for 4 h, cultures grown without xylose reached an OD_{600} of ~0.6, and the cells exhibited normal rod morphology (Fig. 6B, inset). In contrast, cultures grown in the presence of 1% xylose reached an OD_{600} of ~0.5 and exhibited a variety of morphological defects (Fig. 6B). Phase-contrast microscopy revealed cell debris and lysed cells that looked like "ghosts" as well as a mix of normal-length and

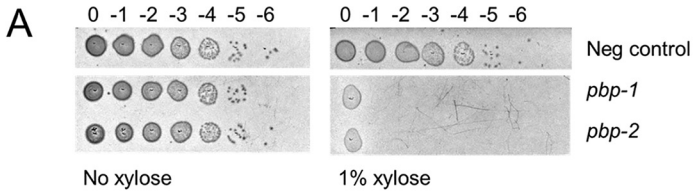

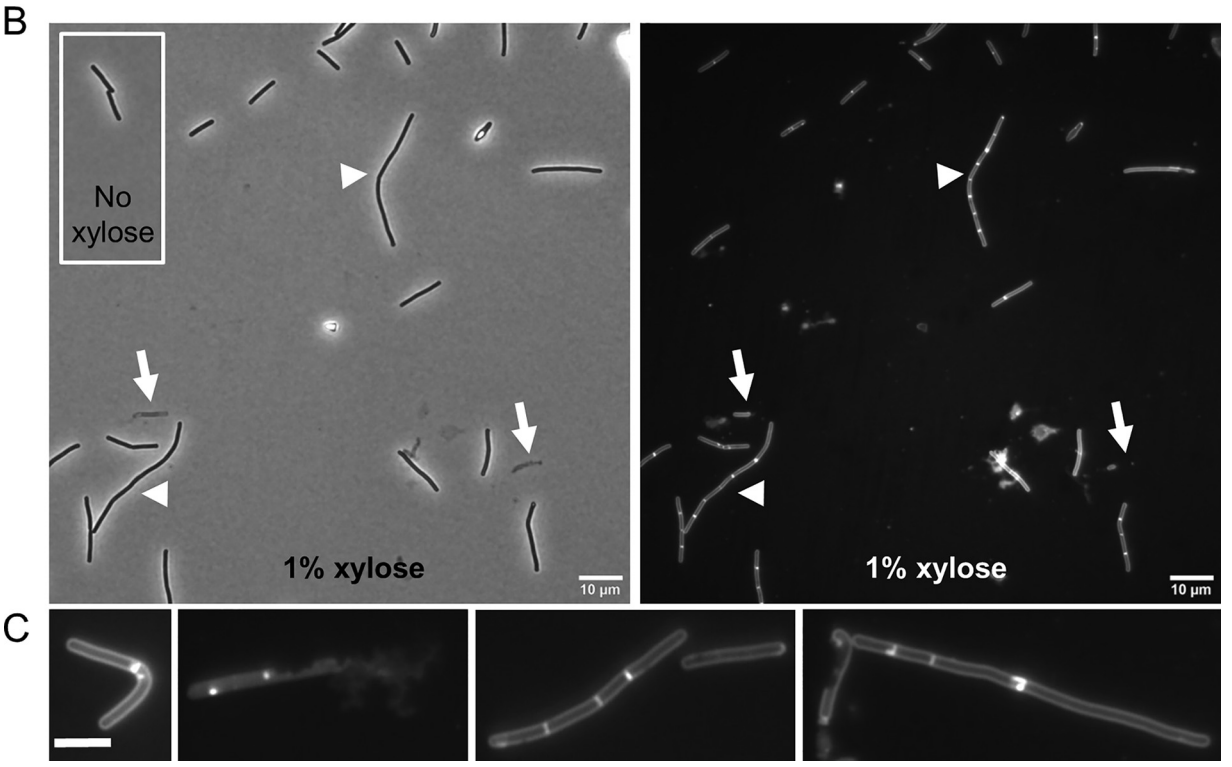

FIG 6 CRISPRi knockdown of *pbp-0712*. (A) Viability assay as described in the legend to Fig. 4. CRISPRi constructs used in this experiment were pIA34 (*neg*^{sgRNA} [negative control]), pIA40 (*pbp-0712-1*^{sgRNA}), and pIA41 (*pbp-0712-2*^{sgRNA}). (B) Cell morphology. A culture of R20291/pIA40 (*pbp-0712-1*^{sgRNA}) grown overnight in TY Thi$_{10}$ medium was inoculated to a starting OD_{600} of 0.05 in TY Thi$_{10}$ medium with or without 1% xylose. After growth for 6 h, cells were stained with the membrane dye FM4-64 and photographed under a phase-contrast (left) or fluorescence (right) microscope. Arrows indicate lysed cells. Arrowheads indicate chained cells. (C) Representative cells showing a variety of morphological defects: bent, lysis, chaining with septa, and elongated cells with few septa. Bar = 10 μm. These results are representative of data from at least two independent experiments.

elongated rods, some of which were bent. Staining with the membrane dye FM4-64 revealed that a few of the filamentous cells had extensive regions lacking division septa, but most were chains of relatively short cells that appeared to have synthesized a division septum but not separated (a "chaining" phenotype). These morphological defects are reminiscent of those observed in a *C. difficile mld* mutant, an operon that has been shown to play a role in cell division and morphology (44). Collectively, they implicate PBP-0712 in elongation, division, and overall integrity of the PG sacculus.

DISCUSSION

In summary, we have built and tested two new tools that we hope will be useful additions to the *C. difficile* molecular biology toolbox. We cloned the regulatory elements of the *C. difficile* xylose utilization operon to generate a xylose-inducible expression plasmid. When driving the expression of *mCherryOpt*, induction is 100-fold or higher and uniform across the population. Bacterial growth was not affected with up to 3% xylose, the highest concentration tested. The lack of inducer toxicity is a potential advantage over existing tetracycline- and nisin-inducible vectors (8, 10). In addition, P_{xyl} can be combined with tetracycline- and/or nisin-inducible promoters to independently regulate the expression of multiple genes in the same cell. Catabolite repression does not appear to be an issue, as the presence of 1% glucose reduced fluorescence by only 40%. A potential caveat is that the consumption of xylose might change the inducer concentration over the course of an experiment, although this issue could presumably be addressed by deleting *xylBA*, which likely encode products necessary for xylose utilization.

We also constructed a CRISPR interference tool for use in *C. difficile*. The CRISPRi plasmid is an *E. coli-C. difficile* shuttle vector that expresses sgRNA constitutively from the P_{gdh} promoter and codon-optimized *dCas9* under the control of P_{xyl}. Repression of gene expression can be tuned by inducing *dCas9* expression with different amounts of xylose. It is relatively easy to target repression to a gene of choice by replacing the 20-nt base-pairing region in the sgRNA with one that is complementary to the gene of interest. Indeed, all of the sgRNAs tested in this study were highly effective (3 targeting *ftsZ*, 2 targeting *slpA*, and 2 targeting *pbp-0712*). We constructed two or three sgRNAs for each target to avoid being misled by off-target effects. The likelihood of different sgRNAs causing the same off-target effect is expected to be minimal.

An important limitation of CRISPRi is polarity on downstream (and, in some cases, upstream) genes (23). In this respect, CRISPRi is inferior to in-frame deletions. Deletion and insertion mutants are also preferable for animal studies, where issues of plasmid stability and the requirement for xylose induction make the current CRISPRi tools a poor fit. These limitations might be overcome in the future by integrating constitutively expressed CRISPRi systems into the chromosome.

Despite these limitations, CRISPRi offers several advantages compared to existing methods for constructing null mutants in *C. difficile*. First, it does not require working in a special *C. difficile* background. Second, it is very fast because targeting a new gene is simply a matter of cloning a new sgRNA. Third, interpreting the effects of gene silencing avoids some of the complications of compensatory changes that might occur during the construction of a gene deletion. A further advantage of CRISPRi is that it can be used to explore the consequences of inactivating essential genes, as illustrated here for *ftsZ* (depletion phenotype, filamentation) and *pbp-0712* (depletion phenotype, a complex mixture of lysis and aberrant morphologies). In fact, after we submitted this study to the review process, Marreddy et al. used CRISPRi to demonstrate that the fatty acid biosynthesis gene *fabK* is essential in *C. difficile* (45). Finally, CRISPRi could be used to tune the expression of a gene of interest to suboptimal levels, with potential applications in drug discovery screens for synthetic phenotypes (23, 46, 47).

MATERIALS AND METHODS

Strains, media, and growth conditions. Bacterial strains are listed in Table 3. *C. difficile* strains used in this study were derived from either 630Δ*erm* or R20291, both of which have been sequenced. *C. difficile* was routinely grown in tryptone-yeast (TY) medium, supplemented as needed with thiampheni-

TABLE 3 Strains used in this study

Strain	Genotype or description	Source or reference
E. coli		
OmniMAX-2 T1^R	F′ [*proAB*$^+$ *lacI*^{q} *lacZ*ΔM15 Tn*10*(Tet^r) Δ(*ccdAB*)] *mcrA* Δ(*mrr-hsdRMS-mcrBC*) ϕ80(*lacZ*)ΔM15 Δ(*lacZYA-argF*)*U169 endA1 recA1 supE44 thi-1 gyrA96 relA1 tonA panD*	Invitrogen
HB101/pRK24	F$^-$ *mcrB mrr hsdS20*(r_B^- m_B^-) *recA13 leuB6 ara-14 proA2 lacY1 galK2 xyl-5 mtl-1 rpsL20*	49
C. difficile		
R20291	Wild-type *C. difficile* strain from UK outbreak (ribotype 027)	
630Δ*erm*	Spontaneous erythromycin-sensitive derivative of strain 630 (ribotype 012)	55
CRG1496	630Δ*erm* Δ*pyrE*	13
UM275	630Δ*erm* with P_{veg}::*rfp* downstream of *pyrE*	This study

col at 10 μg/ml (Thi_{10}), kanamycin at 50 μg/ml, or cefoxitin at 16 μg/ml. TY medium consisted of 3% tryptone, 2% yeast extract, and 2% agar (for solid medium). *C. difficile* strains were maintained at 37°C in an anaerobic chamber (Coy Laboratory Products) in an atmosphere of 10% H_2, 5% CO_2, and 85% N_2.

Escherichia coli strains were grown in LB medium at 37°C with chloramphenicol at 10 μg/ml or ampicillin at 100 μg/ml as needed. LB medium contained 1% tryptone, 0.5% yeast extract, 0.5% NaCl, and, for plates, 1.5% agar.

Plasmid and strain construction. All plasmids are listed in Table 4; an expanded version of this table which includes additional information relevant to plasmid assembly is provided in Table S1 in the supplemental material. Plasmids were constructed by isothermal assembly (48) using reagents from New England Biolabs (Ipswich, MA). Regions of plasmids constructed using PCR were verified by DNA sequencing. The oligonucleotide primers used in this work were synthesized by Integrated DNA Technologies (Coralville, IA) and are listed in Table S2. All plasmids were propagated using OmniMax 2-T1R as the cloning host, transformed into HB101/pRK24 (49), and then introduced into *C. difficile* strains by conjugation (50).

Plasmid pAP114 is a P_{xyl}::*mCherryOpt* expression vector derived from pDSW1728 (P_{tet}::*mCherryOpt*) (51). The *tetR*-P_{tet} regulatory element was removed from pDSW1728 by digestion with SacI and BamHI and replaced with a *xylR*-P_{xyl} DNA fragment obtained by PCR of R20291 chromosomal DNA.

TABLE 4 Plasmids used in this study

Plasmid	Relevant feature(s)	Reference
pJK02	P_{tet}::*Cas9-opt* P_{gdh}::sgRNA *colE1 CD6 ori RP4oriT-traJ catP*	12
pJMP2	P_{veg}::sgRNA *colE1 catP amp spc*	23
pJMP4	P_{veg}::*rfp colE1 catP amp spc*	23
pRPF185	*E. coli-C. difficile* shuttle vector with a tetracycline-inducible promoter; P_{tet}::*gusA tetR CD6ori RP4oriT-traJ pMB1ori catP*	7
pdCas9_bacteria	P_{tet}::*dCas9 tetR ori15A catP*	20
pMTL-YN1C	*E. coli-C. difficile* shuttle vector for inserting genes into the *C. difficile* chromosome while restoring *pyrE*; *colE1 RP4oriT-traJ CB102ori-repH′ catP*	13
pDSW1728	P_{tet}::*mCherryOpt catP*	51
pDSW1963	P_{veg}::*rfp catP*	This study
pIA17	P_{veg}::*rfp* in pMTL-YN1C *catP*	This study
pCE531	P_{tet}::*dCas9 catP*	This study
pIA18	P_{tet}::*dCas9* P_{sigA}::sgRNA-*neg catP*	This study
pIA19	$P_{xylB'}$::*mCherryOpt catP*	This study
pAP114	P_{xyl}::*mCherryOpt catP*	This study
pIA20	$P_{xylB'}$::*dCas9* P_{sigA}::sgRNA-*neg catP*	This study
pIA21	P_{xyl}::*dCas9* P_{sigA}::sgRNA-*neg catP*	This study
pIA24	P_{xyl}::*dCas9* P_{veg}::sgRNA-*neg catP*	This study
pIA25	P_{xyl}::*dCas9* P_{gdh}::sgRNA-*neg catP*	This study
pIA26	P_{xyl}::*dCas9* P_{sigA}::sgRNA-*rfp catP*	This study
pIA27	P_{xyl}::*dCas9* P_{veg}::sgRNA-*rfp catP*	This study
pIA28	P_{xyl}::*dCas9* P_{gdh}::sgRNA-*rfp catP*	This study
pIA33	P_{xyl}::*dCas9-opt* P_{gdh}::sgRNA-*rfp catP*	This study
pIA34	P_{xyl}::*dCas9-opt* P_{gdh}::sgRNA-*neg catP*	This study
pIA35	P_{xyl}::*dCas9-opt* P_{gdh}::sgRNA-*ftsZ-1 catP*	This study
pIA36	P_{xyl}::*dCas9-opt* P_{gdh}::sgRNA-*ftsZ-2 catP*	This study
pIA37	P_{xyl}::*dCas9-opt* P_{gdh}::sgRNA-*ftsZ-3 catP*	This study
pIA38	P_{xyl}::*dCas9-opt* P_{gdh}::sgRNA-*slpA-1 catP*	This study
pIA39	P_{xyl}::*dCas9-opt* P_{gdh}::sgRNA-*slpA-2 catP*	This study
pIA40	P_{xyl}::*dCas9-opt* P_{gdh}::sgRNA-*pbp-1 catP*	This study
pIA41	P_{xyl}::*dCas9-opt* P_{gdh}::sgRNA-*pbp-2 catP*	This study

CRISPRi plasmids, including the final construct, pIA33, were built on the backbone of pRPF185 (7), an *E. coli-C. difficile* shuttle vector with a chloramphenicol resistance marker and the conjugation locus $RP4_{oriT\text{-}traJ}$. Initial constructs harbored *dCas9* from *S. pyogenes* that was amplified from pdCas9_bacteria (20). The final construct, pIA33, harbored *dCas9* with codons optimized for *C. difficile*. This was achieved by amplifying codon-optimized *Cas9* from pJK02 (12) with primers designed such that the active-site residues Asp10 and His840 were changed to alanines. Both versions of *dCas9* were placed under P_{xyl} control. Single guide RNA (sgRNA) targeting *rfp* was based on the sequence shown to be effective in *B. subtilis* (23) and cloned under the control of three different constitutive promoters: a synthetic promoter that we termed P_{sigA} (29, 52), P_{veg} (amplified from pJMP2 [23]), and P_{gdh} (amplified from pJK02 [12]), yielding pIA26, pIA27, and pIA28, respectively. The final construct, pIA33, included sgRNA under the control of P_{gdh}. Negative-control plasmids (pIA25 for *dCas9* and pIA34 for *dCas9-opt*) had the base-pairing sequence of the sgRNA replaced by 20 nucleotides that do not anneal next to a PAM.

The algorithm provided by Benchling (53) was used to design sgRNAs targeting *ftsZ*, *slpA*, and *cdr20291_0712*, the last of which codes for a penicillin-binding protein referred to as PBP-0712 (or *pbp-0712*) in this study. Guide parameters were set to default conditions to identify a 20-nucleotide guide with the PAM set to NGG. Final candidates were selected to be high scoring and bind to the nontemplate strand in the first one-third of the gene sequence. The sequences for sgRNAs are summarized in Table S3.

We constructed a derivative of *C. difficile* 630Δ*erm* that expresses red fluorescent protein (*rfp*) from the P_{veg} promoter and is in a single copy on the chromosome. This enabled an easy quantitative readout to evaluate our initial, exploratory CRISPRi plasmids. The strain was constructed by allelic exchange (13) using *C. difficile* CRG1496 (630Δ*erm* Δ*pyrE*) as a *pyrE*-deficient recipient and plasmid pIA17 to cross-in P_{veg}::*rfp* while reconstituting a functional *pyrE* gene.

Xylose induction. Cultures of R20291 or 630Δ*erm* harboring pAP114 grown overnight were subcultured to an OD_{600} of 0.05 and grown in the presence of various xylose concentrations at 37°C. Once cultures reached an OD_{600} of about 0.5 (approximately 5 h), cultures were fixed, and fluorescence was quantitated in a plate reader or by flow cytometry. Experiments to evaluate CRISPRi constructs targeting *rfp* followed the same growth protocol unless noted otherwise.

Fixation protocol. Cells were fixed as previously described (10, 44). Briefly, a 500-μl aliquot of cells in growth medium was added directly to a microcentrifuge tube containing 120 μl of a 5× fixation cocktail: 100 μl of a 16% (wt/vol) paraformaldehyde aqueous solution (Alfa Aesar, Ward Hill, MA) and 20 μl of 1 M $NaPO_4$ buffer (pH 7.4). The sample was mixed, removed from the Coy chamber, and incubated at room temperature in the dark for 60 min. The fixed cells were washed three times with phosphate-buffered saline (PBS), resuspended in 110 μl of PBS, and left in the dark for a minimum of 3 h to allow for chromophore maturation.

Microscopy. Microscopy was performed as described previously (10). Cells were immobilized using thin agarose pads (1%). Phase-contrast and fluorescence micrographs were recorded on an Olympus BX60 microscope equipped with a 100× UPlanApo objective (numerical aperture, 1.35). For FM4-64 red fluorescence, the filter set (catalog no. 41004; Chroma Technology Corp., Brattleboro, VT) comprised a 538- to 582-nm excitation filter, a 595-nm dichroic mirror (long pass), and a 582- to 682-nm emission filter. Micrographs were captured with a Hamamatsu Orca Flash 4.0 $V2^+$ complementary metal oxide semiconductor (CMOS) camera.

Staining membranes with FM4-64. When membrane morphology was evaluated, cells were stained with the lipophilic dye FM4-64 (Life Technologies). For this, 50 μl of the cell culture was removed from the anaerobic chamber and pelleted by centrifugation. After 45 μl of the supernatant was discarded, the pellet was resuspended in the remaining culture fluid, and 2 μl of 0.05 mg/ml FM4-64 was added. Cells were then imaged directly, with no washing steps.

Flow cytometry. Cells were analyzed at the Flow Cytometry Facility at the University of Iowa using the Becton, Dickinson LSR II instrument with a 561-nm laser, a 610/20-nm-band-pass filter, and a 600 LP dichroic filter as previously described (10). Data were analyzed using BD FACSDiva software.

Fluorescence measurements with a plate reader. The Infinite M200 Pro plate reader (Tecan, Research Triangle Park, NC) was used to measure bulk samples from cultures as described previously (10). Fixed cells in PBS (100 μl) were added to the wells of a 96-well microtiter plate (black, flat optical bottom). Fluorescence was recorded as follows: excitation at 554 nm, emission at 610 nm, and gain setting at 160 to evaluate plasmid-based expression of *mCherryOpt* or at 220 to evaluate *rfp* expression from a single, chromosomal copy. The cell density (OD_{600}) was also recorded and used to normalize the fluorescence reading.

Viability assay. Initial evaluation of CRISPRi targeting *ftsZ*, *slpA*, and *pbp-0712* was performed by making a serial dilution of a culture grown overnight and spotting 5 μl on TY Thi_{10} agar with and without 1% xylose. Plates were photographed after overnight incubation (~18 h).

Evaluation of SlpA levels. S-layer proteins were extracted using low-pH glycine as described previously (33). Briefly, 40 ml TY Thi_{10} medium was inoculated at a 1:50 dilution with a culture grown overnight, and the culture was grown for 8 h with and without 1% xylose. Cells were removed from the anaerobic chamber, pelleted, and washed with 10 ml PBS. Washed pellets were resuspended in 400 μl 0.2 M glycine (pH 2.2) and agitated gently on a tube rotator at room temperature for 30 min. Samples were neutralized with 1 M Tris-HCl (pH 8.8) and analyzed by SDS-PAGE using standard methods. Whole-cell samples for analysis by SDS-PAGE were prepared by pelleting 1 ml of a stationary-phase culture, resuspending the culture in 80 μl Laemmli buffer, and heating the mixture to 95°C for 5 min.

MIC determination. Sensitivity to lysozyme was determined by preparing a dilution series of lysozyme (catalog no. L38100; RPI) in a 96-well plate in 50 μl TY Thi_{10} medium with concentrations

ranging from 0.5 to 32 mg/ml. Wells were inoculated with 50 μl of a diluted culture suspension (10^6 CFU/ml; OD_{600} of roughly 0.005) and grown at 37°C for 17 h, exposing cells to a lysozyme concentration range of 0.25 to 16 mg/ml. Unfortunately, high lysozyme concentrations (1 mg/ml or higher) in TY medium turn sufficiently turbid to prevent a direct readout of cell growth by the optical density. Instead, CFU were determined as follows. A 10-μl sample from each well was diluted 10-fold by adding the sample to a daughter plate containing 90 μl TY medium per well. From this, 5 μl was spotted onto TY agar and incubated for 20 to 24 h. The MIC was considered to be the lowest concentration of lysozyme at which 5 or fewer colonies were found.

Sporulation assay. Determination of sporulation efficiency was performed according to an established protocol (54), with minor modifications. An aliquot (30 μl) of a culture grown overnight was struck (5 cm) on TY Thi_{10} plates with or without 1% xylose. After 24 h of growth at 37°C, cells were scraped into 600 μl PBS and vortexed thoroughly. A 300-μl aliquot was removed from the anaerobic chamber, heated to 60°C for 30 min to kill vegetative cells, and returned to anaerobic conditions. A 10-fold dilution series in TY medium was generated from both the untreated and the heat-treated aliquots, followed by spotting 5 μl onto TY agar plates amended with 0.1% taurocholate and 0.1% cysteine to promote the germination of spores. The sporulation efficiency was calculated as the viability of the heat-treated samples divided by the viability of the untreated samples.

Accession number(s). The DNA sequences of plasmids in Fig. 1 have been submitted to GenBank and are available under accession no. MK368760 (pAP114) and MK368761 (pIA33).

SUPPLEMENTAL MATERIAL

Supplemental material for this article may be found at https://doi.org/10.1128/JB.00711-18.

SUPPLEMENTAL FILE 1, PDF file, 1.7 MB.

ACKNOWLEDGMENTS

This work was supported by National Institutes of Health grants R01AI087834 (C.D.E.) and R21AI121576 (C.D.E. and D.S.W.) from the National Institute of Allergy and Infectious Diseases and by a development grant to D.S.W. from the Department of Microbiology and Immunology at the University of Iowa. Some data presented here were obtained at the Flow Cytometry Facility, which is a Carver College of Medicine/Holden Comprehensive Cancer Center core research facility at the University of Iowa. The facility is funded through user fees and the generous financial support of the Carver College of Medicine, Holden Comprehensive Cancer Center, and Iowa City Veteran's Administration Medical Center.

Plasmid pdCas9-bacteria was a gift from Stanley Qi (Addgene plasmid 44249). We thank Joe Sorg for pJK02, Jason Peters for pJMP2 and pJMP4, Nigel Minton for pMTL-YN1C, and members of the Ellermeier and Weiss laboratories for helpful discussions.

REFERENCES

1. Lessa FC, Mu Y, Bamberg WM, Beldavs ZG, Dumyati GK, Dunn JR, Farley MM, Holzbauer SM, Meek JI, Phipps EC, Wilson LE, Winston LG, Cohen JA, Limbago BM, Fridkin SK, Gerding DN, McDonald LC. 2015. Burden of *Clostridium difficile* infection in the United States. N Engl J Med 372:825–834. https://doi.org/10.1056/NEJMoa1408913.
2. Abt MC, McKenney PT, Pamer EG. 2016. *Clostridium difficile* colitis: pathogenesis and host defence. Nat Rev Microbiol 14:609–620. https://doi.org/10.1038/nrmicro.2016.108.
3. Leffler DA, Lamont JT. 2015. *Clostridium difficile* infection. N Engl J Med 372:1539–1548. https://doi.org/10.1056/NEJMra1403772.
4. Shen A. 2012. *Clostridium difficile* toxins: mediators of inflammation. J Innate Immun 4:149–158. https://doi.org/10.1159/000332946.
5. Kyne L, Hamel MB, Polavaram R, Kelly CP. 2002. Health care costs and mortality associated with nosocomial diarrhea due to *Clostridium difficile*. Clin Infect Dis 34:346–353. https://doi.org/10.1086/338260.
6. CDC. 2013. Antibiotic resistance threats in the United States, 2013. CDC, Atlanta, GA.
7. Fagan RP, Fairweather NF. 2011. *Clostridium difficile* has two parallel and essential Sec secretion systems. J Biol Chem 286:27483–27493. https://doi.org/10.1074/jbc.M111.263889.
8. Purcell EB, McKee RW, McBride SM, Waters CM, Tamayo R. 2012. Cyclic diguanylate inversely regulates motility and aggregation in *Clostridium difficile*. J Bacteriol 194:3307–3316. https://doi.org/10.1128/JB.00100-12.
9. McBride SM, Sonenshein AL. 2011. Identification of a genetic locus responsible for antimicrobial peptide resistance in *Clostridium difficile*. Infect Immun 79:167–176. https://doi.org/10.1128/IAI.00731-10.
10. Ransom EM, Weiss DS, Ellermeier CD. 2016. Use of mCherryOpt fluorescent protein in *Clostridium difficile*. Methods Mol Biol 1476:53–67. https://doi.org/10.1007/978-1-4939-6361-4_5.
11. Heap JT, Cartman ST, Kuehne SA, Cooksley C, Minton NP. 2010. ClosTron-targeted mutagenesis. Methods Mol Biol 646:165–182. https://doi.org/10.1007/978-1-60327-365-7_11.
12. McAllister KN, Bouillaut L, Kahn JN, Self WT, Sorg JA. 2017. Using CRISPR-Cas9-mediated genome editing to generate *C. difficile* mutants defective in selenoproteins synthesis. Sci Rep 7:14672. https://doi.org/10.1038/s41598-017-15236-5.
13. Ng YK, Ehsaan M, Philip S, Collery MM, Janoir C, Collignon A, Cartman ST, Minton NP. 2013. Expanding the repertoire of gene tools for precise manipulation of the *Clostridium difficile* genome: allelic exchange using *pyrE* alleles. PLoS One 8:e56051. https://doi.org/10.1371/journal.pone.0056051.
14. Kim L, Mogk A, Schumann W. 1996. A xylose-inducible *Bacillus subtilis* integration vector and its application. Gene 181:71–76. https://doi.org/10.1016/S0378-1119(96)00466-0.
15. Meisenzahl AC, Shapiro L, Jenal U. 1997. Isolation and characterization of a xylose-dependent promoter from *Caulobacter crescentus*. J Bacteriol 179:592–600. https://doi.org/10.1128/jb.179.3.592-600.1997.
16. Wieland KP, Wieland B, Götz F. 1995. A promoter-screening plasmid and

xylose-inducible, glucose-repressible expression vectors for *Staphylococcus carnosus*. Gene 158:91–96. https://doi.org/10.1016/0378-1119(95)00137-U.
17. Nariya H, Miyata S, Kuwahara T, Okabe A. 2011. Development and characterization of a xylose-inducible gene expression system for *Clostridium perfringens*. Appl Environ Microbiol 77:8439–8441. https://doi.org/10.1128/AEM.05668-11.
18. Choudhary E, Thakur P, Pareek M, Agarwal N. 2015. Gene silencing by CRISPR interference in mycobacteria. Nat Commun 6:6267. https://doi.org/10.1038/ncomms7267.
19. Liu X, Gallay C, Kjos M, Domenech A, Slager J, van Kessel SP, Knoops K, Sorg RA, Zhang JR, Veening JW. 2017. High-throughput CRISPRi phenotyping identifies new essential genes in *Streptococcus pneumoniae*. Mol Syst Biol 13:931. https://doi.org/10.15252/msb.20167449.
20. Qi LS, Larson MH, Gilbert LA, Doudna JA, Weissman JS, Arkin AP, Lim WA. 2013. Repurposing CRISPR as an RNA-guided platform for sequence-specific control of gene expression. Cell 152:1173–1183. https://doi.org/10.1016/j.cell.2013.02.022.
21. Sato'o Y, Hisatsune J, Yu L, Sakuma T, Yamamoto T, Sugai M. 2018. Tailor-made gene silencing of *Staphylococcus aureus* clinical isolates by CRISPR interference. PLoS One 13:e0185987. https://doi.org/10.1371/journal.pone.0185987.
22. Tan SZ, Reisch CR, Prather KLJ. 2018. A robust CRISPR interference gene repression system in *Pseudomonas*. J Bacteriol 200:e00575-17. https://doi.org/10.1128/JB.00575-17.
23. Peters JM, Colavin A, Shi H, Czarny TL, Larson MH, Wong S, Hawkins JS, Lu CHS, Koo BM, Marta E, Shiver AL, Whitehead EH, Weissman JS, Brown ED, Qi LS, Huang KC, Gross CA. 2016. A comprehensive, CRISPR-based functional analysis of essential genes in bacteria. Cell 165:1493–1506. https://doi.org/10.1016/j.cell.2016.05.003.
24. Gu Y, Ding Y, Ren C, Sun Z, Rodionov DA, Zhang W, Yang S, Yang C, Jiang W. 2010. Reconstruction of xylose utilization pathway and regulons in Firmicutes. BMC Genomics 11:255. https://doi.org/10.1186/1471-2164-11-255.
25. Gärtner D, Degenkolb J, Ripperger JA, Allmansberger R, Hillen W. 1992. Regulation of the *Bacillus subtilis* W23 xylose utilization operon: interaction of the Xyl repressor with the *xyl* operator and the inducer xylose. Mol Gen Genet 232:415–422.
26. Sizemore C, Wieland B, Götz F, Hillen W. 1992. Regulation of *Staphylococcus xylosus* xylose utilization genes at the molecular level. J Bacteriol 174:3042–3048. https://doi.org/10.1128/jb.174.9.3042-3048.1992.
27. Antunes A, Martin-Verstraete I, Dupuy B. 2011. CcpA-mediated repression of *Clostridium difficile* toxin gene expression. Mol Microbiol 79:882–899. https://doi.org/10.1111/j.1365-2958.2010.07495.x.
28. Antunes A, Camiade E, Monot M, Courtois E, Barbut F, Sernova NV, Rodionov DA, Martin-Verstraete I, Dupuy B. 2012. Global transcriptional control by glucose and carbon regulator CcpA in *Clostridium difficile*. Nucleic Acids Res 40:10701–10718. https://doi.org/10.1093/nar/gks864.
29. Helmann JD. 1995. Compilation and analysis of *Bacillus subtilis* sigma A-dependent promoter sequences: evidence for extended contact between RNA polymerase and upstream promoter DNA. Nucleic Acids Res 23:2351–2360. https://doi.org/10.1093/nar/23.13.2351.
30. Caspi R, Altman T, Billington R, Dreher K, Foerster H, Fulcher CA, Holland TA, Keseler IM, Kothari A, Kubo A, Krummenacker M, Latendresse M, Mueller LA, Ong Q, Paley S, Subhraveti P, Weaver DS, Weerasinghe D, Zhang P, Karp PD. 2014. The MetaCyc database of metabolic pathways and enzymes and the BioCyc collection of pathway/genome databases. Nucleic Acids Res 42:D459–D471. https://doi.org/10.1093/nar/gkt1103.
31. Caspi R, Billington R, Ferrer L, Foerster H, Fulcher CA, Keseler IM, Kothari A, Krummenacker M, Latendresse M, Mueller LA, Ong Q, Paley S, Subhraveti P, Weaver DS, Karp PD. 2016. The MetaCyc database of metabolic pathways and enzymes and the BioCyc collection of pathway/genome databases. Nucleic Acids Res 44:D471–D480. https://doi.org/10.1093/nar/gkv1164.
32. Dembek M, Barquist L, Boinett CJ, Cain AK, Mayho M, Lawley TD, Fairweather NF, Fagan RP. 2015. High-throughput analysis of gene essentiality and sporulation in *Clostridium difficile*. mBio 6:e02383-14. https://doi.org/10.1128/mBio.02383-14.
33. Kirk JA, Gebhart D, Buckley AM, Lok S, Scholl D, Douce GR, Govoni GR, Fagan RP. 2017. New class of precision antimicrobials redefines role of *Clostridium difficile* S-layer in virulence and viability. Sci Transl Med 9:eaah6813. https://doi.org/10.1126/scitranslmed.aah6813.
34. Erickson HP, Anderson DE, Osawa M. 2010. FtsZ in bacterial cytokinesis: cytoskeleton and force generator all in one. Microbiol Mol Biol Rev 74:504–528. https://doi.org/10.1128/MMBR.00021-10.
35. Xiao J, Goley ED. 2016. Redefining the roles of the FtsZ-ring in bacterial cytokinesis. Curr Opin Microbiol 34:90–96. https://doi.org/10.1016/j.mib.2016.08.008.
36. Elhadi D, Lv L, Jiang XR, Wu H, Chen GQ. 2016. CRISPRi engineering *E. coli* for morphology diversification. Metab Eng 38:358–369. https://doi.org/10.1016/j.ymben.2016.09.001.
37. Mückl A, Schwarz-Schilling M, Fischer K, Simmel FC. 2018. Filamentation and restoration of normal growth in *Escherichia coli* using a combined CRISPRi sgRNA/antisense RNA approach. PLoS One 13:e0198058. https://doi.org/10.1371/journal.pone.0198058.
38. Fagan RP, Fairweather NF. 2014. Biogenesis and functions of bacterial S-layers. Nat Rev Microbiol 12:211–222. https://doi.org/10.1038/nrmicro3213.
39. Fagan RP, Albesa-Jove D, Qazi O, Svergun DI, Brown KA, Fairweather NF. 2009. Structural insights into the molecular organization of the S-layer from *Clostridium difficile*. Mol Microbiol 71:1308–1322. https://doi.org/10.1111/j.1365-2958.2009.06603.x.
40. de la Riva L, Willing SE, Tate EW, Fairweather NF. 2011. Roles of cysteine proteases Cwp84 and Cwp13 in biogenesis of the cell wall of *Clostridium difficile*. J Bacteriol 193:3276–3285. https://doi.org/10.1128/JB.00248-11.
41. Kirby JM, Ahern H, Roberts AK, Kumar V, Freeman Z, Acharya KR, Shone CC. 2009. Cwp84, a surface-associated cysteine protease, plays a role in the maturation of the surface layer of *Clostridium difficile*. J Biol Chem 284:34666–34673. https://doi.org/10.1074/jbc.M109.051177.
42. Typas A, Banzhaf M, Gross CA, Vollmer W. 2011. From the regulation of peptidoglycan synthesis to bacterial growth and morphology. Nat Rev Microbiol 10:123–136. https://doi.org/10.1038/nrmicro2677.
43. Sauvage E, Kerff F, Terrak M, Ayala JA, Charlier P. 2008. The penicillin-binding proteins: structure and role in peptidoglycan biosynthesis. FEMS Microbiol Rev 32:234–258. https://doi.org/10.1111/j.1574-6976.2008.00105.x.
44. Ransom EM, Williams KB, Weiss DS, Ellermeier CD. 2014. Identification and characterization of a gene cluster required for proper rod shape, cell division, and pathogenesis in *Clostridium difficile*. J Bacteriol 196:2290–2300. https://doi.org/10.1128/JB.00038-14.
45. Marreddy R, Wu X, Madhab S, Prior AM, Jones J, Sun D, Hevener KE, Hurdle JG. 2019. The fatty acid synthesis protein enoyl-ACP reductase II (FabK) is a target for narrow-spectrum antibacterials for *Clostridium difficile* infection. ACS Infect Dis 5:208–217. https://doi.org/10.1021/acsinfecdis.8b00205.
46. Abrahams GL, Kumar A, Savvi S, Hung AW, Wen S, Abell C, Barry CE, III, Sherman DR, Boshoff HI, Mizrahi V. 2012. Pathway-selective sensitization of *Mycobacterium tuberculosis* for target-based whole-cell screening. Chem Biol 19:844–854. https://doi.org/10.1016/j.chembiol.2012.05.020.
47. Jost M, Chen Y, Gilbert LA, Horlbeck MA, Krenning L, Menchon G, Rai A, Cho MY, Stern JJ, Prota AE, Kampmann M, Akhmanova A, Steinmetz MO, Tanenbaum ME, Weissman JS. 2017. Combined CRISPRi/a-based chemical genetic screens reveal that rigosertib is a microtubule-destabilizing agent. Mol Cell 68:210.e6–223.e6. https://doi.org/10.1016/j.molcel.2017.09.012.
48. Gibson DG, Young L, Chuang RY, Venter JC, Hutchison CA, III, Smith HO. 2009. Enzymatic assembly of DNA molecules up to several hundred kilobases. Nat Methods 6:343–345. https://doi.org/10.1038/nmeth.1318.
49. Trieu-Cuot P, Arthur M, Courvalin P. 1987. Origin, evolution and dissemination of antibiotic resistance genes. Microbiol Sci 4:263–266.
50. Kirk JA, Fagan RP. 2016. Heat shock increases conjugation efficiency in *Clostridium difficile*. Anaerobe 42:1–5. https://doi.org/10.1016/j.anaerobe.2016.06.009.
51. Ransom EM, Ellermeier CD, Weiss DS. 2015. Use of mCherry red fluorescent protein for studies of protein localization and gene expression in *Clostridium difficile*. Appl Environ Microbiol 81:1652–1660. https://doi.org/10.1128/AEM.03446-14.
52. Moran CP, Jr, Lang N, LeGrice SF, Lee G, Stephens M, Sonenshein AL, Pero J, Losick R. 1982. Nucleotide sequences that signal the initiation of transcription and translation in *Bacillus subtilis*. Mol Gen Genet 186:339–346. https://doi.org/10.1007/BF00729452.
53. Benchling. 2018. Biology software. Benchling, San Francisco, CA.
54. Shen A, Fimlaid KA, Pishdadian K. 2016. Inducing and quantifying *Clostridium difficile* spore formation. Methods Mol Biol 1476:129–142. https://doi.org/10.1007/978-1-4939-6361-4_10.
55. Hussain HA, Roberts AP, Mullany P. 2005. Generation of an erythromycin-sensitive derivative of *Clostridium difficile* strain 630 (630Δ*erm*) and demonstration that the conjugative transposon Tn*916*ΔE enters the genome of this strain at multiple sites. J Med Microbiol 54:137–141. https://doi.org/10.1099/jmm.0.45790-0.